Cardinal Exponential Splines: Part I—Theory and Filtering Algorithms

Michael Unser, *Fellow, IEEE,* and Thierry Blu, *Member, IEEE*

***Abstract*—Causal exponentials play a fundamental role in classical system theory. Starting from those elementary building blocks, we propose a complete and self-contained signal processing formulation of exponential splines defined on a uniform grid. We specify the corresponding B-spline basis functions and investigate their reproduction properties (Green function and exponential polynomials); we also characterize their stability (Riesz bounds). We show that the exponential B-spline framework allows an exact implementation of continuous-time signal processing operators including convolution, differential operators, and modulation, by simple processing in the discrete B-spline domain. We derive efficient filtering algorithms for multiresolution signal extrapolation and approximation, extending earlier results for polynomial splines. Finally, we present a new asymptotic error formula that predicts the magnitude and the Nth-order decay of the L_2-approximation error as a function of the knot spacing T.**

***Index Terms*—Continuous-time signal processing, convolution, differential operators, Green functions, interpolation, modulation, multiresolution approximation, splines.**

I. Introduction

During the past decade, there has been an increasing number of papers devoted to the use of polynomial splines in signal processing (cf. [1] and the references therein). The interest in these techniques grew after it was shown that most classical spline-fitting problems on a uniform grid (interpolation, least squares, and smoothing splines) could be solved efficiently using recursive digital filtering techniques [2]–[4]. These spline-based algorithms have been found to be quite advantageous for image processing and medical imaging, especially in the context of high-quality interpolation, where it has been demonstrated that they yield the best cost-quality tradeoff among all linear techniques [5]–[8]. Polynomial splines have also been shown to play a fundamental role in wavelet theory [9].

Although there are a few applications of polynomial splines in continuous-time signal processing [10]–[12], splines have apparently had less impact in this area. Part of the reason may be that (piecewise) polynomials do only appear marginally in basic systems theory (e.g., the rect function and the impulse response of the $(n+1)$-fold integrator: $t_+^n/n!$). The most prominent functions in continuous-time signal-and-systems theory are the exponentials, which correspond to the modes of differential systems (analog filters and circuits) [13]. Having made this observation and motivated by the search for a unification between the continuous and discrete-time approaches to signal processing, we decided to undertake the task of extending the previously mentioned formulation to the enlarged class of exponential splines. These splines, as their name suggests, are made up of exponential segments that are connected together in a smooth fashion. They form a natural extension of the polynomial splines and have been characterized mathematically in relatively general terms [14], [15]. Even though there have not been many computational applications of exponential splines so far, we believe that they constitute an attractive, unifying framework for signal processing, which is something that we intend to demonstrate in the present series of papers. Two earlier papers by Panda *et al.* [17] and Asahi *et al.* [37] are also relevant to the issue.

The kind of splines that are the most appropriate for signal processing are the *cardinal* ones, which are defined on a uniform grid. Mathematically, this corresponds to the simplest possible setup, which goes back to the pioneering work of Schoenberg on polynomial splines in 1946 [17]. Since then, there have been many theoretical advances, and the methods of spline constructions have been extended for nonuniform grids and many other types of nonpolynomial basis functions [14]. In particular, there is a small, rather sophisticated mathematical literature on exponential splines [15], [18], [19], which are themselves special cases of Tchebycheffian splines [20], [21], as well as L-splines [22]. There are also a few papers on exponential box splines [23], [24], which are multidimensional extensions of the univariate B-splines; however, this is relatively advanced material because the mathematical analysis of multivariate box splines is known to be much harder than in the univariate case [25]. These unifying spline theories are very elegant, but their level of generality is often such that it is difficult for a spline outsider to extract the information that is relevant to his application.

As far as signal processing is concerned, what is missing in the literature is a specialized, accessible, and yet comprehensive theory of cardinal exponential splines, and this is the gap that this paper is attempting to fill. The good news is that the choice of a uniform grid leads to important simplifications, thus making it possible to propose a self-contained formulation using relatively elementary mathematics, which is something that has not been done before, to the best of our knowledge. The main advantages of the cardinal framework are as follows.

- *Shift-invariance:* The structure of the problem is such that we can make use of the standard mathematical tools of signal processing (Fourier, Laplace, and z-transforms), which simplifies the formulation considerably.

Manuscript received November 26, 2003; revised April 16, 2004. This work was supported in part by Grant 200020–101821 of the Swiss National Science Foundation. The associate editor coordinating the review of this manuscript and approving it for publication was Prof. Karim Drouiche.

The authors are with the Biomedical Imaging Group, EPFL, CH-1015 Lausanne, Switzerland (e-mail: michael.unser@epfl.ch; Thierry.Blu@epfl.ch).

Digital Object Identifier 10.1109/TSP.2005.843700

- *Digital filter-based solutions:* Similar to what has been done before for polynomial splines [3], [4], it is possible to derive explicit formulae and recursive digital filtering solutions that do not exist in the more general, nonuniform, or multidimensional cases.
- *Terminology:* The concepts and algorithms can be explained in standard "signal-and-systems" terms, making these splines more accessible to this community.

The paper is organized as follows. In Section II, we start with a brief review of ordinary differential operators and show how these can be linked to the definition of exponential splines. From there, we focus on cardinal splines, which are defined with respect to the integer grid. In Section III, we investigate the properties of the exponential B-splines and prove that every cardinal spline has a unique and stable representation in terms of such basis functions. In the process, we also provide B-spline reproduction formulae for Green functions and exponential polynomials, as well as an explicit specification of the Gram sequence of the B-spline basis. In Section IV, we show that the exponential B-spline framework is ideally suited for performing some basic continuous-time signal processing operations in the discrete domain. In particular, we present novel digital algorithms for the exact implementation of continuous-time convolution, differential operators, dilation, and modulation. Finally, in Section V, we consider the possibility of changing the spline resolution and describe a filtering algorithm for computing the minimum-error approximation of a signal in some cardinal spline space with step T. We also provide an asymptotic formula for the L_2-approximation error for smooth signals.

The practical relevance of these results will be demonstrated in a series of companion papers [26], which are part of a larger program that aims at unifying continuous and discrete signal processing.

A. Notations

Vectors are marked with an arrow and are used to represent N-tuples, i.e., $\vec{u} = (u_1, u_2, \ldots, u_N)$. The concatenation of two vectors $\vec{u}$ and $\vec{v}$ of size N and M, respectively, yields a vector of size $N+M$ denoted by $(\vec{u} : \vec{v}) = (u_1, \ldots, u_N, v_1, \ldots, v_M)$.

We consider real or complex-valued continuously defined signals $f(t)$, $t \in \mathbb{R}$ that are typically included in $L_2(R)$, which is the Hilbert space of finite-energy functions. The corresponding (Hermitian) inner product is $\langle f(\cdot), g(\cdot)\rangle = \int_{-\infty}^{+\infty} f(t)g^*(t)\,\mathrm{d}t$, where $g^*(t)$ is the complex conjugate of $g(t)$. $\|f\|_{L_2} = \sqrt{\langle f, f\rangle}$ is the L_2-norm of f.

The Fourier transform of $f(t)$ is denoted by $\hat{f}(\omega)$. For $f(t) \in L_2(R) \cap L_1(R)$, it is given by $\hat{f}(\omega) = \int_{-\infty}^{+\infty} f(t)e^{-j\omega t}\,\mathrm{d}t$; otherwise, it is defined in the distributional sense. The (unilateral) Laplace transform of a causal (possibly exponentially increasing) function $f(t)$ is defined as $\mathcal{L}\{f\} = F(s) = \int_0^{\infty} f(t)e^{-st}\mathrm{d}t$. When $F(s)$ is analytical along the axis $s = j\omega$, then $F(j\omega) = \hat{f}(\omega)$ coincides with the Fourier transform.

The one-sided power function is $t_+^n = \max\{t, 0\}^n$. The unit step is written as $1_+(t)$, which is compatible with this notation.

The discrete counterpart of $L_2(R)$ is ℓ_2, which is the Hilbert space of square-summable (real or complex-valued) sequences. The discrete signal $a[k]$, $k \in \mathbb{Z}$ is characterized by its z-transform $A(z) = \sum_{k\in\mathbb{Z}} a[k]z^{-k}$. Its discrete-time Fourier transform $A(e^{j\omega}) = \sum_{k\in\mathbb{Z}} a[k]e^{-j\omega k}$ is obtained by setting $z = e^{j\omega}$.

II. Preliminaries

In this section, we briefly review some basic properties of ordinary differential operators and use these to define of a wide class of exponential splines.

A. Differential Operators

Let us consider the generic differential operator of order N

$$\mathrm{L}\{f\} = \mathrm{D}^N\{f\} + a_{N-1}\mathrm{D}^{N-1}\{f\} + \cdots + a_0\mathrm{I}\{f\} \qquad (1)$$

with constant coefficients $a_n \in \mathbb{C}$, whose argument is some continuously varying time function $f = f(t)$. Here, $\mathrm{D}^n = \mathrm{d}^n/\mathrm{d}t^n$ denotes the nth-order derivative, and $\mathrm{I} = \mathrm{D}^0$ is the identity operator. The operator L is also characterized by the roots of its characteristic polynomial

$$L(s) = s^N + a_{N-1}s^{N-1} + \cdots + a_0 = \prod_{n=1}^{N}(s - \alpha_n). \qquad (2)$$

We will therefore use the notation $\mathrm{L}_{\vec{\alpha}}$, where $\vec{\alpha} = (\alpha_1, \alpha_2, \ldots, \alpha_N)$ is a vector that specifies the roots explicitly. Note that the roots may be complex and that their ordering is irrelevant; in other words, there is an equivalence class associated with all possible permutations of the components of $\vec{\alpha}$. In order to be able to handle the case of multiple roots, we will sometimes use the alternative notation $\{\alpha_{(m)}\}_{m=1,\ldots,N_d}$, where $\alpha_{(m)}$ stands for the mth distinct root which is of order (or multiplicity) $n_{(m)}$. Thus, we have that $\sum_{m=1}^{N_d} n_{(m)} = N$, where N_d is the total number of distinct roots.

The equation $y(t) = \mathrm{L}_{\vec{\alpha}}\{x(t)\}$ (where $x(t)$ and $y(t)$ are the input and output signals, respectively) defines a linear, shift-invariant system (convolution operator). Knowing the roots of the characteristic polynomial, we can factorize the system into a cascade of first-order operators $\mathrm{L}_{\vec{\alpha}} = (\mathrm{D}-\alpha_1\mathrm{I})*\cdots*(\mathrm{D}-\alpha_N\mathrm{I})$. In the Fourier domain, this is expressed by

$$L_{\vec{\alpha}}(j\omega) = \prod_{n=1}^{N}(j\omega - \alpha_n) = \prod_{m=1}^{N_d}(j\omega - \alpha_{(m)})^{n_{(m)}} \qquad (3)$$

where the right-hand side form of the frequency response uses our second, alternative root notation. Note that the above formula corresponds to the evaluation of the characteristic polynomial (2) for $s = j\omega$.

B. Null Space

The null space of $\mathrm{L}_{\vec{\alpha}}$, which is denoted by $\mathcal{N}_{\vec{\alpha}}$, is the space of dimension N that contains all the solutions of the homogenous differential equation $\mathrm{L}_{\vec{\alpha}}\{x_0(t)\} = 0$. As is well known from systems theory, these can all be written as linear combinations

of the modes of $\mathrm{L}_{\vec{\alpha}}$, which are exponentials and, possibly, exponential polynomials of the form $e^{\alpha t}, t\,e^{\alpha t}, \ldots, t^{m-1}e^{\alpha t}$ for a root of multiplicity m. More precisely, we have that

$$\mathcal{N}_{\vec{\alpha}} = \mathrm{span}\{t^{n-1}e^{\alpha_{(m)}t}\}_{m=1,\ldots,N_d;\ n=1,\ldots,n_{(m)}}$$

where the $\alpha_{(m)}$'s are the N_d distinct roots of the characteristic polynomial (2). This means that $\mathrm{L}_{\vec{\alpha}}$ has an exponential annihilation property in that it will produce a zero output for any excitation signal $x_0(t) \in \mathcal{N}_{\vec{\alpha}}$.

C. Green Function

In signal processing, a shift-invariant operator is usually characterized by its impulse response $h(t) = \mathrm{L}\{\delta(t)\}$. When dealing with differential equations, it is more convenient mathematically to consider the reverse characterization $\delta(t) = \mathrm{L}\{\rho(t)\}$, where $\rho(t)$ is the so-called *Green function* of L. In signal processing terms, $\rho(t)$ is the impulse response of the inverse operator L^{-1}. The only difficulty when dealing with the differential operator $\mathrm{L}_{\vec{\alpha}}$ is that $\rho(t)$ is not unique in the sense that we may add to it any component $x_0(t) \in \mathcal{N}_{\vec{\alpha}}$ and still satisfy the equation $\delta(t) = \mathrm{L}_{\vec{\alpha}}\{\rho(t) + x_0(t)\}$. To obtain a unique definition, it is therefore necessary to introduce additional (boundary) conditions. Among all possible solutions, there is a single one that is causal (i.e., $\rho_{\vec{\alpha}}(t) = 0, \forall t < 0$), and it is the one that we are considering here.

It is well known that the Green function of the first-order operator $\mathrm{L}_\alpha = \mathrm{D} - \alpha\mathrm{I}$ is the one-sided (or causal) exponential:

$$\rho_\alpha(t) = 1_+(t) \cdot e^{\alpha t} \tag{4}$$

as can be verified by substitution. We can then use this result and work our way up to higher orders using the fact that $\mathrm{L}_{\vec{\alpha}}^{-1} = (\mathrm{D} - \alpha_1\mathrm{I})^{-1} * \cdots * (\mathrm{D} - \alpha_N\mathrm{I})^{-1}$, which follows from the (commutative) factorization of $\mathrm{L}_{\vec{\alpha}}$ into a cascade of first-order systems. This leads to the convolution formula for the Green function of $\mathrm{L}_{\vec{\alpha}}$

$$\rho_{\vec{\alpha}}(t) = \left(\rho_{\alpha_1} * \rho_{\alpha_2} * \cdots * \rho_{\alpha_N}\right)(t) \tag{5}$$

which is guaranteed to be causal (but not necessarily absolutely integrable), provided that the individual constituents are causal as well. To obtain the corresponding explicit time formula, we take the Laplace transform of (5) and decompose it into partial fractions

$$\frac{1}{L_{\vec{\alpha}}(s)} = \prod_{m=1}^{N_d} \frac{1}{(s-\alpha_{(m)})^{n_{(m)}}} = \sum_{m=1}^{N_d}\sum_{n=1}^{n_{(m)}} \frac{c_{m,n}}{(s-\alpha_{(m)})^n} \tag{6}$$

which imposes the coefficients $c_{m,n}$. Finally, we take the inverse transform, which yields

$$\rho_{\vec{\alpha}}(t) = \sum_{m=1}^{N_d}\sum_{n=1}^{n_{(m)}} c_{m,n}\frac{t_+^{n-1}}{(n-1)!}e^{\alpha_{(m)}t}. \tag{7}$$

D. Exponential Splines

We will now see how it is possible to associate a family of exponential splines with each differential operator $\mathrm{L}_{\vec{\alpha}}$. This is a generalization of the classical polynomial-spline case which corresponds to the choice $\mathrm{L}_{(0,\ldots,0)} = \mathrm{D}^N$.

Definition 1: An exponential spline with parameter $\vec{\alpha}$ and knots $-\infty < \cdots t_k < t_{k+1} < \cdots < +\infty$ is a function $s(t)$ such that

$$\mathrm{L}_{\vec{\alpha}}\{s(t)\} = \sum_k a_k\delta(t-t_k) \tag{8}$$

where the sequence a_k is bounded and where $\delta(t)$ is the Dirac distribution.

This means that $s(t)$ exhibits discontinuities of order N at the knot points t_k but that it is very smooth otherwise; in fact, in each interval, $s(t)$ coincides with a function that is in the null space of $\mathrm{L}_{\vec{\alpha}}$. From the definition of the Green function, we deduce the following explicit representation of the exponential spline:

$$s(t) = \sum_k a_k\rho_{\vec{\alpha}}(t-t_k) + p_0(t) \tag{9}$$

where $p_0(t)$ is an additional global component that is a solution of the homogeneous differential equation $\mathrm{L}_{\vec{\alpha}}\{p_0(t)\} = 0$. Note that in order to characterize $s(t)$ uniquely, we need to determine the homogenous component $p_0(t) \in \mathcal{N}_{\vec{\alpha}}$; this is usually done through the specification of boundary conditions (N linear constraints).

An important property of the exponential polynomials is that the space that they span is shift invariant; specifically, for any shift τ, we have that

$$\begin{aligned}(t-\tau)^n e^{\alpha(t-\tau)} &= \sum_{m=0}^{n}\binom{n}{m}t^m(-\tau)^{n-m}e^{-\alpha\tau}e^{\alpha t}\\ &= \sum_{m=1}^{n} a_{\tau,m}\,t^m e^{\alpha t}\end{aligned}$$

which is also an exponential polynomial with parameter α. Consequently, since the individual spline atoms (shifted Green functions and $p_0(t)$) are linear combinations of exponential polynomials (the modes of $\mathrm{L}_{\vec{\alpha}}$), the same is obviously true for $s(t)$ within each interval $[t_k, t_{k+1}]$. Moreover, Definition 1 implies that the spline pieces are patched together in a way that guarantees the continuity of the function and its derivatives up to order $(N-2)$. These are properties that justify the denomination "exponential spline."

The present spline definition is quite general. For $\vec{\alpha} = (0, 0, \ldots, 0)$, we recover the classical—nonuniform—polynomial splines, which are extremely well studied and the most popular in applications [27], [28]. For $\vec{\alpha} = (0, 0, -\alpha, \alpha)$, we get the splines under tension, which were initially derived from the solution of a variational problem [29]. For $\vec{\alpha} = (\vec{\alpha}_0 : -\vec{\alpha}_0) \in \mathbb{R}^N$, the null space $\mathcal{N}_{\vec{\alpha}}$ contains pairs of real exponential functions $(e^{\alpha t}, e^{-\alpha t})$ that can be grouped and represented in terms of the hyperbolic functions $(\cosh(\alpha t), \sinh(\alpha t))$; this is the reason why these types of splines are often referred to as *hyperbolic* ones [18], [30]. The *trigonometric* splines are another important family for which the roots are purely imaginary and equally spaced around the origin [31], [32].

On the other hand, the exponential splines that have just been presented are a special case of the so-called Tchebycheffian splines (or T-splines), which are made of segments coinciding with functions in certain Tchebycheffian spaces (here, the exponential polynomials) that are connected together such as to insure a certain degree of continuity [20], [21]. These latter splines are themselves included in the family of L-splines, which can also be represented in terms of the Green function of some general differential operator L [22]. The theory of L-splines goes quite further than what has been exposed here in that the differential operators L may be shift-variant. In fact, L is defined by a formula analogous to (1) with coefficients $a_n = a_n(t)$ that may vary smoothly with t [14].

III. Cardinal Exponential Splines

The *cardinal exponential splines* correspond to the specialized case where the knots are at the integer, i.e., $t_k = k$. We will now see that this particular framework allows for important simplifications and that it is ideally suited for a signal processing formulation. While the general spline representation (9) is obviously still valid in this particular context, it is not the one that we are promoting here. Instead, we will consider an equivalent expansion in terms of compactly supported basis functions, which is much more efficient to work with. Interestingly, the computational tools that we will describe are, for the most part, based on digital-filtering techniques.

A. Construction of Exponential B-Splines

The exponential B-splines are localized, that is compactly supported and shortest possible, versions of the Green functions that generate the exponential splines. The way in which such B-splines are constructed is especially easy to understand in the first-order case and is illustrated in Fig. 1. One takes $\rho_\alpha(t)$ and subtracts a shifted—and properly weighted—version of it to annihilate the exponential term for $t \geq 1$. This yields the first order B-spline with parameter α

$$\beta_\alpha(t) = \rho_\alpha(t) - e^\alpha \rho_\alpha(t-1). \tag{10}$$

Note that this first-order B-spline is supported in [0,1), irrespective of $\alpha \in \mathbb{C}$. In addition, it is non-negative, provided that ρ_α is not oscillating, that is, when α is real.

The higher order B-splines are obtained by successive convolution of lower order ones:

$$\beta_{\vec{\alpha}}(t) = \left(\beta_{\alpha_1} * \beta_{\alpha_2} * \cdots * \beta_{\alpha_N}\right)(t) \tag{11}$$

which is a process that is justified by the convolution relation (5) of the corresponding Green functions. It follows that the Nth-order B-splines are supported in $[0, N)$. Another important property is that the regularity of these functions increases with N; indeed, $\beta_{\vec{\alpha}}(t) \in C^{N-2}$ (the class of functions with continuous derivatives up to order $N-2$), which is not surprizing since it is an Nth-order exponential spline, as we will see below. Some examples of such B-splines are shown in Fig. 2.

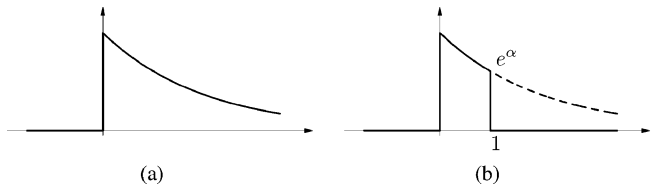

Fig. 1. From Green functions to B-splines. (a) Causal exponential $\rho_\alpha(t)$ with $\alpha = -0.5$. (b) Exponential B-spline $\beta_\alpha(t)$.

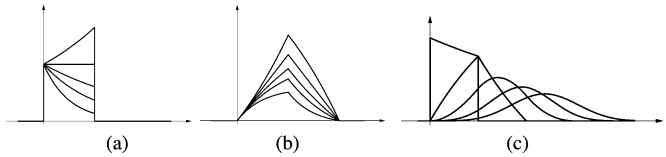

Fig. 2. Examples of exponential B-splines. (a) First-order B-splines with $\alpha = -2, -1, -1/2, 0$, and 1/2. (b) Second-order B-splines $\beta_{(0,\alpha)}(t)$ with α as in (a). (c) Nth-order B-splines $\beta_{(\alpha,\ldots,\alpha)}(t)$ with $\alpha = -1/4$ and $N = 1, \ldots, 5$.

As in the first-order case, the higher order exponential B-splines are non-negative whenever $\vec{\alpha}$ is a real vector. In fact, we have the following inequality:

$$\forall \vec{\alpha} \in \mathbb{C}^N, \quad |\beta_{\vec{\alpha}}(t)| \leq \beta_{\mathrm{Re}(\vec{\alpha})}(t) \tag{12}$$

which can be proven by induction.

We now define the localization operator with parameter $\vec{\alpha}$ as

$$\Delta_{\vec{\alpha}}\{f(t)\} = \sum_{k=0}^{N} d_{\vec{\alpha}}[k] f(t-k) \tag{13}$$

where $d_{\vec{\alpha}}[k]$ is the Nth-order exponential finite-difference sequence characterized by its z-transform

$$\Delta_{\vec{\alpha}}(z) = \prod_{n=1}^{N} (1 - e^{\alpha_n} z^{-1}).$$

Thanks to this notation, the exponential B-spline with parameter $\vec{\alpha}$ can be written explicitly and more concisely as

$$\beta_{\vec{\alpha}}(t) = \Delta_{\vec{\alpha}}\{\rho_{\vec{\alpha}}(t)\}. \tag{14}$$

Thus, we have established that the exponential B-spline can be expressed as a linear combination of integer shifts of the Green function $\rho_{\vec{\alpha}}(t)$, which proves that it is a cardinal exponential spline with parameter $\vec{\alpha}$.

Another convenient way to characterize these B-splines is to go to the Fourier domain. By combining the Fourier transforms of (11) and (10)—or, equivalently, by transforming (14)—we find that

$$\hat{\beta}_{\vec{\alpha}}(\omega) = \prod_{n=1}^{N} \frac{1 - e^{\alpha_n - j\omega}}{j\omega - \alpha_n} = \frac{\Delta_{\vec{\alpha}}(e^{j\omega})}{L_{\vec{\alpha}}(j\omega)}. \tag{15}$$

Since $\hat{\beta}_{\vec{\alpha}}(\omega)$ is formed from a product of first-order terms, it is of interest to investigate the general behavior of its individual components. The frequency response of the first-order B-spline

with complex parameter $\alpha = \sigma + j\omega_0$, $\hat{\beta}_{\sigma+j\omega_0}(\omega)$ is a sinc-like function that exhibits a well-pronounced maximum at the resonance frequency $\omega_0 = \mathrm{Im}(\alpha)$ and that asymptotically decays like $O(|\omega - \omega_0|^{-1})$ as one moves away from it. The amplitude of the maximum is

$$M_\alpha = \begin{cases} 1, & \text{for } \mathrm{Re}(\alpha) = 0 \\ \frac{e^{\mathrm{Re}(\alpha)}-1}{\mathrm{Re}(\alpha)}, & \text{for } \mathrm{Re}(\alpha) \neq 0 \end{cases} \tag{16}$$

and can be used to normalize the amplitude response. To prove this, it suffices to notice that $|\hat{\beta}_{\sigma+j\omega_0}(\omega)| \leq \int_{-\infty}^{+\infty} |\beta_{\sigma+j\omega_0}(t)|dt = \int_0^1 e^{\sigma t}dt = M_\alpha$ and that this maximum is attained for $\omega = \omega_0$. Interestingly, the general shape of the normalized frequency response only depends on the magnitude of $\sigma = \mathrm{Re}(\alpha)$ but not on its sign.

The frequency response for the limiting case $\mathrm{Re}(\alpha) = 0$ is a modulated sinc function, which exhibits zeros at $\omega = \mathrm{Im}(\alpha) + 2\pi k$, with $k \neq 0$. The general effect of including an attenuation term $\mathrm{Re}(\alpha) \neq 0$ is to broaden the central peak and to smooth out the response, as illustrated in Fig. 3. Our next result formalizes the property that the central peak at ω_0 is the narrowest—and the attenuation away from it maximal—for $\sigma = 0$.

Proposition 1: The general inequality

$$\forall \omega \in \mathbb{R}, \quad \frac{|\hat{\beta}_\alpha(\omega)|}{\sup\limits_{w\in\mathbb{R}} |\hat{\beta}_\alpha(w)|} \geq \frac{|\hat{\beta}_{j\mathrm{Im}(\alpha)}(\omega)|}{\sup\limits_{w\in\mathbb{R}} |\hat{\beta}_{j\mathrm{Im}(\alpha)}(w)|} = |\hat{\beta}_{j\mathrm{Im}(\alpha)}(\omega)| \tag{17}$$

holds true for all $\alpha \in \mathbb{C}$.

Proof: Starting from (15) with $N = 1$ and $\alpha = \sigma + j\omega_0$, we write the following identity, which is obtained after a few trigonometric manipulations:

$$\left|\frac{\hat{\beta}_{\sigma+j\omega_0}(\omega)}{\hat{\beta}_{j\omega_0}(\omega)}\right|^2 = M_\sigma^2 \cdot \frac{\left|\sin\left(\frac{\omega-\omega_0}{2}\right)\right|^{-2} + \left|\sinh\left(\frac{\sigma}{2}\right)\right|^{-2}}{\left|\frac{\omega-\omega_0}{2}\right|^{-2} + \left|\frac{\sigma}{2}\right|^{-2}}.$$

The right-hand side is seen to be larger than $M_\sigma^2 = \sup\limits_{\omega\in\mathbb{R}} |\hat{\beta}_\alpha(\omega)|^2$, thanks to the general inequalities

$$|\sin x|^{-2} \geq x^{-2} + \frac{1}{3} \quad \text{and} \quad |\sinh x|^{-2} \geq x^{-2} - \frac{1}{3}.$$

These two relations are proven by noticing that $\arcsin(x) - x(1 - x^2/3)^{-1/2}$ and $\mathrm{arcsinh}(x) - x(1 + x^2/3)^{-1/2}$ are increasing functions of x (their derivative is always positive) and are thus themselves positive for $x \geq 0$. ∎

Note that this result obviously implies that $|\hat{\beta}_{j\mathrm{Im}(\vec{\alpha})}(\omega)| \leq |\hat{\beta}_{\vec{\alpha}}(\omega)|/M_{\vec{\alpha}} \leq 1$, with the extended vector notation $M_{\vec{\alpha}} = \prod_{n=1}^N M_{\alpha_n}$.

B. B-Spline Properties

The B-splines are always stable and well-defined (i.e., bounded and compactly supported), even when the underlying Green functions are diverging at infinity (as in the polynomial spline case); that is, when there is at least one root with $\mathrm{Re}(\alpha) \geq 0$. In fact, changing the sign of the roots has a simple mirroring (and scaling) effect

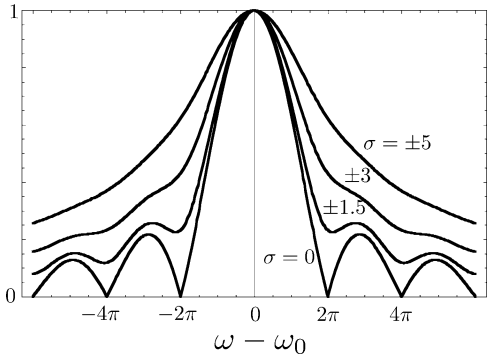

Fig. 3. Normalized first-order frequency responses $|\hat{\beta}_{\sigma+j\omega_0}(\omega)|/M_\sigma$ for various values of σ. These functions all have their maximum at $\omega = \omega_0$. The lowest curve is $|\hat{\beta}_{j\omega_0}(\omega)|$, which vanishes at all integer multiples of 2π, except at the origin ω_0, where it takes the value one.

$$\beta_{-\vec{\alpha}}(t) = \left(\prod_{n=1}^N e^{-\alpha_n}\right) \beta_{\vec{\alpha}}(-t + N) \tag{18}$$

which is a property that can be visualized in Fig. 2(a) for the first-order case. A direct implication is that an exponential B-spline is symmetric with respect to its centerline whenever its roots are either zero or can be grouped in pairs of opposite sign; a prototypical example is that $\beta_{(0,\alpha,-\alpha)}(t + t_0) = \beta_{(0,\alpha,-\alpha)}(-t + t_0)$ with $t_0 = 3/2$. In addition, note that one can increase the multiplicity of the nonzero roots in the previous example to generate a one-parameter family of symmetric B-splines that is equivalent to the generalized B-splines considered in [16].

The convolution of two B-splines yields another one of augmented order:

$$\left(\beta_{\vec{\alpha}_1} * \beta_{\vec{\alpha}_2}\right)(t) = \beta_{(\vec{\alpha}_1:\vec{\alpha}_2)}(t) \tag{19}$$

which is a key property that follows directly from (11). There is a corresponding formula for the cross-correlation of two B-splines

$$\begin{aligned} \langle \beta_{\vec{\alpha}_1}(\cdot), \beta_{\vec{\alpha}_2}(\cdot - \tau)\rangle &= \left(\beta_{\vec{\alpha}_1} * \beta^H_{\vec{\alpha}_2}\right)(\tau) \\ &= \left(\prod_{n=1}^{N_2} e^{\alpha^*_{2,n}}\right) \beta_{(\vec{\alpha}_1:-\vec{\alpha}^*_2)}(\tau + N_2) \end{aligned} \tag{20}$$

with the notation $h^H(t) = h^*(-t)$. This is established by using (18) and noticing that $\beta^H_{\vec{\alpha}_2}(t) = \beta_{\vec{\alpha}^*_2}(-t)$.

Another fundamental property is that $\beta_{\vec{\alpha}}(t)$ is the shortest possible cardinal spline with exponential parameter $\vec{\alpha}$. This can be established by adapting Schoenberg's famous proof for the polynomial spline case [33]. One intuitive explanation is the following: A localization filter of order N has N zeros that precisely cancel the poles of the denominator in (15). If the localization filter was chosen to be shorter, there would be some singularities left, and the basis functions would be infinitely supported. If, on the other hand, one would select a longer, pole-cancelling filter, it would necessarily include $\Delta_{\vec{\alpha}}(z)$ as a

factor and, therefore, yield a longer basis function that would include the B-spline as a convolutional factor.

C. B-Spline Representation

The key result that is emphasized in this section is the B-spline representation theorem, which is a generalization of Schoenberg's classical result for cardinal polynomial splines [33].

Theorem 1: The set of functions $\{\beta_{\vec{\alpha}}(t-k)\}_{k\in\mathbb{Z}}$ provides a Riesz basis of $V_{\vec{\alpha}}$ —the space of cardinal exponential splines with finite energy—if and only if $\alpha_n - \alpha_m \neq j2\pi k, k \in \mathbb{Z}$ for all pairs of distinct, purely imaginary roots.

Thus, if one excludes the pathological cases of improperly spaced imaginary roots first identified by Ron [24], this means that every cardinal exponential spline with parameter $\vec{\alpha} = (\alpha_1, \ldots, \alpha_N)$ has a unique and stable representation in terms of its B-spline expansion

$$s(t) = \sum_{k\in\mathbb{Z}} c[k]\, \beta_{\vec{\alpha}}(t-k). \tag{21}$$

Even though this result can be deduced from existing theorems in spline theory (e.g., in the context of the construction of local bases for L-splines [14] or in the multidimensional setting of exponential box splines [23], [24]), we will propose our own derivation, which will reveal some important connections and relations that will be particularly useful for our purpose, which is signal processing.

There are two important aspects to Theorem 1. The first is *completeness*, meaning that the B-splines span the space of cardinal exponential splines. To prove this point, we need to show that in the case of integer knots, it is possible to express the individual components in (9)—shifted Green functions and exponential polynomials—as linear combinations of exponential B-splines. The second is *stability*, which presupposes the existence of upper and lower Riesz bounds. Here, we use Fourier analysis techniques that are now well established in sampling and wavelet theory [34], [35] and obtain some precise estimates, which have not been reported before.

1) Reproduction of the Green Function: Formally, we can reconstruct the Green function $\rho_{\vec{\alpha}}(t)$ by inverting (14), which yields

$$\rho_{\vec{\alpha}}(t) = \Delta_{\vec{\alpha}}^{-1}\{\beta_{\vec{\alpha}}(t)\} = \sum_{k=0}^{+\infty} p_{\vec{\alpha}}[k]\, \beta_{\vec{\alpha}}(t-k) \tag{22}$$

where $p_{\vec{\alpha}}[k]$ is the unique causal sequence that satisfies $p_{\vec{\alpha}}[k] * d_{\vec{\alpha}}[k] = \delta[k]$. Thus, the z-transform of $p_{\vec{\alpha}}[k]$ is $P_{\vec{\alpha}}(z) = \Delta_{\vec{\alpha}}^{-1}(z)$, which we decompose as

$$\begin{aligned} P_{\vec{\alpha}}(z) &= \frac{1}{\Delta_{\vec{\alpha}}(z)} = \prod_{m=1}^{N_d} \frac{1}{(1-e^{\alpha_{(m)}} z^{-1})^{n_{(m)}}} \\ &= \sum_{m=1}^{N_d} \sum_{n=1}^{n_{(m)}} \frac{c'_{m,n}}{(1-e^{\alpha_{(m)}} z^{-1})^{n}} \end{aligned} \tag{23}$$

where the $c'_{m,n}$ are coefficients determined using the standard partial-fraction expansion method. Next, we apply the inverse z-transform, which yields an explicit formula for the Green-function reproducing sequence in (22):

$$p_{\vec{\alpha}}[k] = \sum_{m=1}^{N_d} \sum_{n=1}^{n_{(m)}} c'_{m,n} \frac{p_{\alpha_{(m)}}^{[n-1]}[k]}{(n-1)!} \tag{24}$$

where

$$p_{\alpha}^{[n]}[k] = \begin{cases} e^{\alpha k}, & \text{for } n = 0 \\ (k+1)(k+2)\ldots(k+n)e^{\alpha k}, & \text{for } n \geq 1 \end{cases}$$

is the discrete analog of the exponential polynomial $t^n e^{\alpha t}$. In the case of a first-order operator, the B-spline coefficients in (22) are the samples of the Green function $\rho_\alpha(t)$, as illustrated in Fig. 4(a).

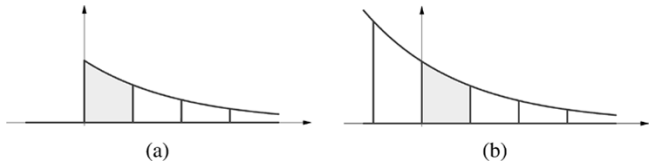

Fig. 4. B-spline reproduction properties. (a) Reproduction of the Green function $\rho_\alpha(t)$. (b) Reproduction of the exponential $e^{\alpha t}$. The B-spline is shaded.

For higher order systems, the principle is essentially the same, except that the determination of the coefficients is slightly more involved.

2) Reproduction of Exponential Polynomials: If we extrapolate the Green function for $t < 0$, that is, if we drop the "+" subscript of t_+ in (7), we get an exponential polynomial. We can obtain the corresponding B-spline reproduction formula by extrapolating (22) for negative k's. In the first-order case, this yields the particularly simple formula

$$e^{\alpha t} = \sum_{k\in\mathbb{Z}} e^{\alpha k} \beta_\alpha(t-k)$$

which is illustrated graphically in Fig. 4(b). Similarly, for a system with a single root α of multiplicity n, we find that

$$t^n e^{\alpha t} = \sum_{k\in\mathbb{Z}} p_\alpha^{[n]}[k]\, \beta_{(\alpha,\ldots,\alpha)}(t-k)$$

which is a generalized version of the well-known monomial reproduction formula of the polynomial B-splines with $\alpha = 0$.

We then extend the argument to higher order splines by observing that the exponential polynomial reproduction is preserved through convolution.

Proposition 2: Let φ_α be a function that reproduces the exponential polynomials in $\mathcal{N}_{(\alpha,\ldots,\alpha)} = \text{span}\{e^{\alpha t}, \ldots, t^p e^{\alpha t}\}$. Then, for any φ such that $\int_{-\infty}^{+\infty} \varphi(t) e^{-\alpha t} \mathrm{d}t \neq 0$, the composite function $\varphi * \varphi_\alpha(t)$ also reproduces these exponential polynomials.

The statement that φ_α reproduces the exponential polynomials of degree p is equivalent to the existence of sequences $p_n[k]$ such that $t^n e^{\alpha t} = \sum_{k\in\mathbb{Z}} p_n[k]\, \varphi_\alpha(t-k)$ for $n = 0, \ldots, p$. For our formulation to be rigorous, we also require two mild technical conditions: i) $\int_{-\infty}^{+\infty} |\varphi(t)\, t^p e^{-\alpha t}| \mathrm{d}t < +\infty$, and ii) $\sum_{k\in\mathbb{Z}} |p_n[k]\, \varphi_\alpha(t-k)| \leq C \cdot |t^n e^{\alpha t}|$, which are satisfied when the functions are exponential B-splines.

Proof: First, we show that the convolution product of $\varphi(t)$ and $t^n e^{\alpha t}$ yields another exponential polynomial of degree n:

$$\begin{aligned}\varphi(t) * t^n e^{\alpha t} &= \int_{-\infty}^{+\infty} \varphi(\tau)(t-\tau)^n e^{\alpha(t-\tau)} \mathrm{d}\tau \\ &= \sum_{k=0}^{n} \binom{n}{k} t^k e^{\alpha t} (-1)^{n-k} \underbrace{\int_{-\infty}^{+\infty} \varphi(\tau) \tau^{n-k} e^{-\alpha\tau} \mathrm{d}\tau}_{m_\varphi^{n-k,\alpha}} \\ &= \sum_{k=0}^{n} b_{n,k} t^k e^{\alpha t}. \end{aligned} \tag{25}$$

The coefficients $b_{n,k}$ are finite because of the decay condition i) on $\varphi(t)$, which ensures that the exponentially weighted moments $m_\varphi^{k,\alpha}$ are well-defined for $k \leq p$.

The next step is to convolve the exponential polynomial reproduction formula of φ_α with φ:

$$\begin{aligned}\varphi(t) * \sum_{k\in\mathbb{Z}} p_n[k] \varphi_\alpha(t-k) &= \sum_{k\in\mathbb{Z}} p_n[k]\, (\varphi * \varphi_\alpha)(t-k) \\ &= \sum_{k=0}^{n} b_{n,k} t^k e^{\alpha t}\end{aligned}$$

where we have made use of (25) and of conditions i) and ii) to justify the exchange of the order of convolution and summation (Fubini's Theorem). Finally, because of our assumption that $m_\varphi^{0,\alpha} \neq 0$, we have that $b_{n,n} \neq 0$ for $n = 0, \ldots, p$, which ensures that these exponential polynomials form a basis of $\mathcal{N}_{(\alpha,\ldots,\alpha)}$. ∎

Since the Nth-order B-spline is constructed by convolution of lower order ones, this implies that it has the ability to reproduce the exponential polynomials that are in the union of the null spaces of all lower order constituents.

Of course, the above argument only holds if the condition of validity for Proposition 1 is met in all cases. This means that we cannot include any first-order B-spline $\varphi = \beta_{\alpha_n}$ for which the condition fails, i.e., $\int_{-\infty}^{+\infty} \beta_{\alpha_n}(t) e^{-\alpha t} \mathrm{d}t = \mathcal{L}\{\beta_{\alpha_n}\}(s)|_{s=\alpha} = 0$, which does only happen when α and α_n are two distinct, purely imaginary roots with $\alpha - \alpha_n = j2\pi k$. In such a situation, the exponential reproduction formula $\sum_{k\in\mathbb{Z}} e^{\alpha k}\, \beta_{\vec{\alpha}}(t-k)$ collapses to zero, implying that the basis functions are linearly dependent. This is a problem that has been studied in depth by Ron [24] within the more general context of exponential box splines.

3) Gram Sequence: The stability of the B-spline basis depends on the condition number of its Gram matrix. Because the basis functions are shifted versions of a single prototype, the Gram matrix is entirely characterized by the Gram (or autocorrelation) sequence

$$\begin{aligned}a_{\vec{\alpha}}[k] &= \langle \beta_{\vec{\alpha}}(\cdot), \beta_{\vec{\alpha}}(\cdot - k) \rangle \\ &= \left(\prod_{n=1}^{N} e^{\alpha_n^*} \right) \beta_{(\vec{\alpha}:-\vec{\alpha}^*)}(k+N)\end{aligned} \tag{26}$$

whose explicit form is obtained as a special case of the cross-correlation formula (20). Note that the Gram sequence is Hermitian-symmetric and that it vanishes for $|k| \geq N$ (remember that $\beta_{(\vec{\alpha}:-\vec{\alpha}^*)}(t)$ is supported in $[0, 2N)$, with its two end points being zero). An important theoretical quantity is the discrete-time Fourier transform of $a_{\vec{\alpha}}[k]$, which can be written in the form of a trigonometric polynomial

$$A_{\vec{\alpha}}(e^{j\omega}) = \sum_{k=-N+1}^{N-1} a_{\vec{\alpha}}[k]\, e^{-j\omega k} \tag{27}$$

the coefficients of which are given by (26). There is also another equivalent form

$$A_{\vec{\alpha}}(e^{j\omega}) = \sum_{n\in\mathbb{Z}} \left| \hat{\beta}_{\vec{\alpha}}(\omega + 2\pi n) \right|^2 \tag{28}$$

which is useful for deriving certain mathematical properties. This latter equation, which is related to the first one through Poisson's summation formula, expresses the fact that $a_{\vec{\alpha}}[k]$ is obtained by sampling the continuously defined autocorrelation function whose Fourier transform is $\left|\hat{\beta}_{\vec{\alpha}}(\omega)\right|^2$.

4) Riesz-Basis Property: The functions $\{\beta_{\vec{\alpha}}(t-k)\}_{k\in\mathbb{Z}}$ are said to form a Riesz basis if and only if there exist two constants $r_{\vec{\alpha}} > 0$ and $R_{\vec{\alpha}} < +\infty$ such that

$$r_{\vec{\alpha}} \cdot \|c\|_{\ell_2} \leq \left\| \sum_{k\in\mathbb{Z}} c[k]\, \beta_{\vec{\alpha}}(t-k) \right\|_{L_2} \leq R_{\vec{\alpha}} \cdot \|c\|_{\ell_2}. \tag{29}$$

Moreover, we know from basic sampling theory that the lower and upper Riesz bounds are given by (cf. [36])

$$r_{\vec{\alpha}} = \inf_{\omega\in[-\pi,\pi]} \sqrt{A_{\vec{\alpha}}(e^{j\omega})} \tag{30}$$

$$R_{\vec{\alpha}} = \sup_{\omega\in[-\pi,\pi]} \sqrt{A_{\vec{\alpha}}(e^{j\omega})} \tag{31}$$

which enables us to compute them on a case-by-case basis by using the expression of $A_{\vec{\alpha}}(e^{j\omega})$ provided by (27).

We now have all the pieces to complete the proof of Theorem 1.

Proof of Theorem 1: The completeness of the B-spline representation is ensured by their reproduction properties (Green function and exponential polynomials) [cf. Sections III.C2 and 3]. To prove the existence of the Riesz bounds for the general Nth-order case, we use the property that $A_{\vec{\alpha}}(e^{j\omega})$ is upper bounded and continuous because $a_{\vec{\alpha}} \in \ell_1$.

The upper bound is taken care immediately by the inequality $R_{\vec{\alpha}}^2 \leq \sum_{k\in\mathbb{Z}} |a_{\vec{\alpha}}[k]| < +\infty$. Because of (28), which represents $A_{\vec{\alpha}}(e^{j\omega})$ as a sum of positive terms, the existence of the lower Riesz bound depends on the structure of the set of frequencies for which $\hat{\beta}_{\vec{\alpha}}(\omega) = 0$. To characterize this set, we define $Z_{k,\vec{\alpha}} = \{\omega \in [0, 2\pi) : \hat{\beta}_{\vec{\alpha}}(\omega + 2\pi k) = 0\}$. Clearly, $Z_{k,\vec{\alpha}} = \bigcup_{n=1}^{N} Z_{k,\alpha_n}$, where the individual Z_{k,α_n}'s are empty, provided that $\mathrm{Re}(\alpha_n) \neq 0$ [cf. the discussion around Fig. 3]. Since $A_{\vec{\alpha}}(e^{j\omega})$ is continuous and bounded, we have a Riesz basis if and only if $A_{\vec{\alpha}}(e^{j\omega}) > 0, \forall\omega \in [0, 2\pi]$, which is equivalent to $\bigcap_{k\in Z} Z_{k,\vec{\alpha}} = \varnothing$. The only potential problem arises when there are some purely imaginary roots. Fortunately, when $\mathrm{Re}(\alpha_n) = 0$, there is always one Z_{k,α_n} that is empty—it corresponds to the segment where sinc takes its maximum value. This leads to an empty intersection over $k \in \mathbb{Z}$ unless there is another distinct, purely imaginary root α_m such that $\alpha_m - \alpha_n =$

$j2\pi k$, which zeroes out the response at the resonance frequency $\omega_n = \mathrm{Im}(\alpha_n)$. ■

5) Some Riesz Bounds: In the simplest first-order case, we have tight upper and lower Riesz bounds

$$r_\alpha = R_\alpha = \sqrt{M_{2\alpha}}$$

which expresses the fact that the corresponding B-spline basis is orthogonal for any $\alpha \in \mathbb{C}$.

More generally, the estimate for the upper Riesz bound $B_{\vec{\alpha}}$, which appears in the proof of Theorem 1, is $\sqrt{\|a_{\vec{\alpha}}\|_{\ell^1}}$. The next proposition is interesting because it allows us to bypass the calculation of (26) and because it leads to the identification of cases for which this upper bound is tight.

Proposition 3: The upper Riesz bound can be estimated by

$$\sup_{\omega\in\mathbb{R}} |\hat{\beta}_{\vec{\alpha}}(\omega)| \le R_{\vec{\alpha}} \le \frac{M_{\vec{\alpha}}}{\sqrt{\max\limits_{n=1,\ldots,N} M_{-|\alpha_n|}}} \tag{32}$$

where $M_{\vec{\alpha}} = \prod_{n=1}^{N} M_{\alpha_n}$ with M_{α_n} defined by (16).

Proof: The left-most inequality is trivial. For the right-most one, we first treat the simpler case $\vec{\alpha} \in \mathbb{R}^N$ (real poles) for which $a_{\vec{\alpha}}[k] \ge 0$ for all k. Our task thus boils down to calculating the corresponding $R^2_{\vec{\alpha}} = \sum_{k\in\mathbb{Z}} \langle \beta_{\vec{\alpha}}(\cdot), \beta_{\vec{\alpha}}(\cdot - k)\rangle$. To this end, we concentrate on the 1-periodic quantity $S_{\vec{\alpha}}(t) = \sum_{k\in\mathbb{Z}} \beta_{\vec{\alpha}}(t-k)$. We pick one component of $\vec{\alpha}$, say α_n, and use the convolution property $\beta_{\vec{\alpha}} = \beta_{\vec{\alpha}'} * \beta_{\alpha_n}$, where $\vec{\alpha}' = \vec{\alpha}\setminus\{\alpha_n\}$. The convolution integral involves the sum $S_{\alpha_n}(t)$, which equals $e^{\alpha_n t}$ for $t \in [0,1)$. This expression is upper bounded by 1 if $\alpha_n < 0$ or by e^{α_n} if $\alpha_n \ge 0$. Then

$$\begin{aligned} S_{\vec{\alpha}}(t) &= S_{\alpha_n}(t) * \beta_{\vec{\alpha}'}(t) \le \sup_t S_{\alpha_n}(t) \cdot \int \beta_{\vec{\alpha}'}(\tau)\,\mathrm{d}\tau \\ &= \sup_t S_{\alpha_n}(t) \cdot \hat{\beta}_{\vec{\alpha}'}(0) \end{aligned}$$

the right-hand side of which is given by $M_{\vec{\alpha}}/M_{\alpha_n}$ if $\alpha_n < 0$, or $(M_{\vec{\alpha}}/M_{\alpha_n}) \cdot e^{\alpha_n} = M_{\vec{\alpha}}/M_{-\alpha_n}$ otherwise. Thus, $S_{\vec{\alpha}}(t) \le M_{\vec{\alpha}}/M_{-|\alpha_n|}$. Finally, by noticing that that $R^2_{\vec{\alpha}} = \langle \beta_{\vec{\alpha}}, S_{\vec{\alpha}}\rangle$ and taking the minimum over the arbitrary component α_n, we get the announced result for the case $\vec{\alpha} \in \mathbb{R}^N$.

When $\vec{\alpha}$ has an imaginary part, we use inequality (12) to show that $\sum_{k\in\mathbb{Z}} \left|\langle \beta_{\vec{\alpha}}(\cdot), \beta_{\vec{\alpha}}(\cdot - k)\rangle\right| \le \sum_{k\in\mathbb{Z}} \langle \beta_{\mathrm{Re}(\vec{\alpha})}(\cdot), \beta_{\mathrm{Re}(\vec{\alpha})}(\cdot - k)\rangle$, which allows us to extend the upper bound to the complex case as well. ■

It is clear from the proof that the upper bound in Proposition 3 is tight whenever the exponential parameters are real, i.e., $\vec{\alpha} \in \mathbb{R}^N$. By using a modulation argument, we see that the same holds true if $\mathrm{Im}(\alpha_n) = \omega_0$, $\forall n$, that is, when all roots are on the same vertical line in the complex plane. Moreover, the right-most estimate in (32) simplifies to $R_{\vec{\alpha}} \le M_{\vec{\alpha}}$, as soon as one of the components of $\vec{\alpha}$ is purely imaginary.

Because of the potential instabilities that have been mentioned before, it is more difficult to obtain in general an estimate for the lower Riesz bound $r_{\vec{\alpha}}$ unless we consider some structured configurations of poles. The next proposition covers the important case where the roots are all included in the same Nyquist region in the complex plane.

Proposition 4: If the roots are such that $\mathrm{Im}(\alpha_n) - \omega_0 \in (-\pi, \pi)$ for all $n = 1, 2, \ldots, N$ and for some radial frequency ω_0, then we have the following lower Riesz-bound estimate:

$$r_{\vec{\alpha}} \ge M_{\vec{\alpha}} \prod_{n=1}^{N} \frac{2\cos\left(\frac{\mathrm{Im}(\alpha_n)-\omega_0}{2}\right)}{\pi + |\mathrm{Im}(\alpha_n) - \omega_0|}. \tag{33}$$

Proof: Without loss of generality, we assume that $\omega_0 = 0$. In that case, we observe that $r_{\vec{\alpha}} \ge \inf_{\omega\in[-\pi,\pi]} |\hat{\beta}_{\vec{\alpha}}(\omega)|$. Next, we apply the inequality provided by Prop. 1, which yields

$$\begin{aligned} r_{\vec{\alpha}} &\ge M_{\vec{\alpha}} \inf_{\omega\in[-\pi,\pi]} |\hat{\beta}_{j\mathrm{Im}(\vec{\alpha})}(\omega)| \\ &\ge M_{\vec{\alpha}} \inf_{\omega\in[-\pi,\pi]} \prod_{n=1}^{N} \left|\mathrm{sinc}\Big(\frac{\omega - \mathrm{Im}(\alpha_n)}{2\pi}\Big)\right|. \end{aligned}$$

Since $\omega \in [-\pi, \pi]$ and $\mathrm{Im}(\alpha_n) \in (-\pi, \pi)$, we are ensured that $\omega - \mathrm{Im}(\alpha_n) \in (-2\pi, 2\pi)$. Moreover, we know that $\mathrm{sinc}(x/2\pi)$ is strictly increasing for $x \in [-2\pi, 0]$ and decreasing for $x \in [0, 2\pi]$. This implies that $\mathrm{sinc}\big((\omega - \mathrm{Im}(\alpha_n))/2\pi\big)$ is minimized either at $\omega = -\pi$ or at $\omega = \pi$, from which we deduce that $\mathrm{sinc}\big((\omega - \mathrm{Im}(\alpha_n))/2\pi\big) \ge 2\cos\big(\mathrm{Im}(\alpha_n)/2\big)/(\pi + |\mathrm{Im}(\alpha_n)|)$. Putting things together, we get our lower bound estimate. ■

Note that the lower bound in (33) vanishes when $\mathrm{Im}(\alpha_n) - \omega_0$ gets closer to $\pm\pi$, which is precisely what happens for the unstable root configurations that have been identified in the proof of Theorem 1.

IV. Continuous/Discrete Signal Processing

In this section, we show how the exponential spline framework that has just been presented can be used advantageously for the exact implementation of a number of fundamental continuous-time signal processing operations. Interestingly, this is achieved by applying standard discrete processing techniques in the B-spline domain. The proposed framework offers an attractive alternative to the traditional bandlimited model, which uses infinitely supported basis functions and is not appropriate for the representation of causal signals.

A. Signal Interpolation

Often, the input signal is given in digital form as a sequence of samples $s[k]$. Thus, the first step of spline processing is to fit the discrete signal with an interpolating spline $s(t)$, specified by its B-spline expansion (21), and such that $s(t)|_{t=k} = s[k]$. This can be achieved quite efficiently by straightforward adaptation of the recursive filtering algorithms that have been proposed for symmetric spline interpolation [4], [37]. For this purpose, we introduce the discrete B-spline sequence $b_{\vec{\alpha}}[k]$, which is obtained by sampling the basis function $\beta_{\vec{\alpha}}(t)$ at the integers. The corresponding z-transform is

$$B_{\vec{\alpha}}(z) = \sum_{k=0}^{N} \beta_{\vec{\alpha}}(k) z^{-k}. \tag{34}$$

The interpolation condition $s(t)|_{t=k} = s[k]$ is equivalent to the discrete convolution relation $s[k] = (b_{\vec{\alpha}} * c)[k]$, which suggests that the B-spline coefficients can be obtained by inverse filtering

of the input signal: $c[k] = (b_{\vec{\alpha}})^{-1} * s[k]$. The z-transform of the inverse filter $(b_{\vec{\alpha}})^{-1}$ can be written as

$$B_{\vec{\alpha}}^{-1}(z) = \frac{1}{\sum_{k=0}^{N} \beta_{\vec{\alpha}}(k) z^{-k}} = \frac{c_0}{\prod_{n=1}^{N}(1 - z_n z^{-1})} \tag{35}$$

where c_0 is a suitable constant and where the z_n's are the zeros of $B_{\vec{\alpha}}(z)$. This is an all-pole, infinite-impulse-response (IIR) filter that is stable, but not necessarily causal, whenever $|z_n| \neq 1$, $\forall n$. A practical way to implement it numerically is to decompose it into a cascade of stable causal and anti-causal filters. The causal part corresponds to the roots $|z_n| < 1$ and is implemented recursively in a conventional fashion. The anti-causal part is associated with the roots $|z_n| > 1$; it is also implemented recursively, but one has to reverse the time axis and to scan the input signal from end to start.

Unfortunately, there is no general guarantee that the interpolation filter (35) is stable unless we are dealing with a Hermitian symmetric B-spline $\beta_{(\vec{\alpha}:-\vec{\alpha}^*)}(t)$, which corresponds to a Gram sequence that satisfies the Riesz-basis condition in Theorem 1. For instance, we can show that the interpolation associated with an odd-order symmetric B-spline $\beta_{(-\vec{\alpha}:0:\vec{\alpha})}(t)$ is unstable because the corresponding filter has a pole at $z = 1$. A standard way around this problem, which is used for odd-order polynomial spline interpolation, is to shift the basis functions (and spline knots) by one half with respect to the grid. In addition, note that for image processing, one prefers to work with basis functions that are centered on the origin, which requires some shifting anyway.

When the interpolation problem is well-posed, or, equivalently, when the interpolation filter is stable, there is a reversible, one-to-one mapping between the signal samples $s[k]$ and the B-spline coefficients $c[k]$. This means that there is no loss of information by representing the signal by its B-spline coefficients, even though the choice of the underlying continuous-time model is somewhat arbitrary, but not more so than the classical bandlimited model (which can also be interpreted as a polynomial spline of infinite order [38], [39]).

B. Convolution

Let $s_1(t) = \sum_{k\in\mathbb{Z}} c_1[k]\beta_{\vec{\alpha}_1}(t-k)$ and $s_2(t) = \sum_{k\in\mathbb{Z}} c_2[k]\beta_{\vec{\alpha}_2}(t-k)$ be two cardinal spline signals with exponential parameter $\vec{\alpha}_1$ and $\vec{\alpha}_2$, respectively. We are interested in evaluating their continuous-time convolution, which we can do explicitly by making use of the B-spline convolution property (19):

$$\begin{aligned}
&s_1(t) * s_2(t) \\
&= \int_{-\infty}^{+\infty} s_1(\tau) s_2(t-\tau) d\tau \\
&= \sum_{k_1\in\mathbb{Z}} \sum_{k_2\in\mathbb{Z}} c_1[k_1] c_2[k_2] \int_{-\infty}^{+\infty} \beta_{\vec{\alpha}_1}(\tau - k_1)\beta_{\vec{\alpha}_2}(t-\tau-k_2) d\tau \\
&= \sum_{k_1\in\mathbb{Z}} \sum_{k\in\mathbb{Z}} c_1[k_1] c_2[k-k_1] \int_{-\infty}^{+\infty} \beta_{\vec{\alpha}_1}(\tau)\beta_{\vec{\alpha}_2}(t-\tau-k) d\tau \\
&= \sum_{k\in\mathbb{Z}} (c_1 * c_2)[k] \beta_{(\vec{\alpha}_1:\vec{\alpha}_2)}(t-k).
\end{aligned} \tag{36}$$

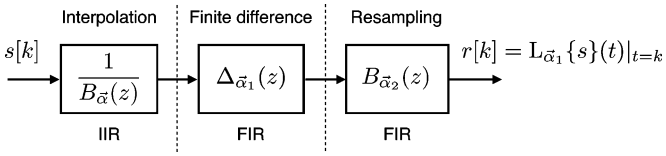

Fig. 5. Signal processing system for the spline-based evaluation of the differential operator $\mathrm{L}_{\vec{\alpha}_1}\{\cdot\}$.

This shows that the continuous-time convolution of two spline signals can be implemented via a discrete convolution of the B-spline coefficients of the underlying signals. The method is exact but requires a change of basis function (augmented-order B-splines).

C. Differential Operators

In line with the previous formula, we choose to partition the B-spline parameter $\vec{\alpha}$ into two subparts $(\vec{\alpha}_1 : \vec{\alpha}_2)$ of length N_1 and N_2, keeping in mind that the ordering of the roots is arbitrary. By considering the Fourier transform representation (15), it is then relatively straightforward to establish the differential relation

$$\mathrm{L}_{\vec{\alpha}_1}\left\{\beta_{(\vec{\alpha}_1:\vec{\alpha}_2)}(t)\right\} = \Delta_{\vec{\alpha}_1}\{\beta_{\vec{\alpha}_2}(t)\} \tag{37}$$

which is the generalization of the well-known multiple differentiation formula of the polynomial B-splines [17]. The important point is that the application of an N_1th-order operator yields a spline of reduced degree $N_2 = N - N_1$, whose B-spline coefficients are the weights associated with the localization operator $\Delta_{\vec{\alpha}_1}$ (exponential finite differences). The restriction, of course, is that the operator must be part of the factorization of $\mathrm{L}_{\vec{\alpha}} = (\mathrm{D} - \alpha_1\mathrm{I}) * \cdots * (\mathrm{D} - \alpha_N\mathrm{I})$. Since the differential operator $\mathrm{L}_{\vec{\alpha}_1}$ is linear and shift-invariant, we can directly transpose the result for an arbitrary spline signal:

$$\begin{aligned}
\mathrm{L}_{\vec{\alpha}_1}\left\{s_{(\vec{\alpha}_1:\vec{\alpha}_2)}(t)\right\} &= \sum_{k\in\mathbb{Z}} c[k]\, \Delta_{\vec{\alpha}_1}\{\beta_{\vec{\alpha}_2}(t-k)\} \\
&= \sum_{k\in\mathbb{Z}} (c * d_{\vec{\alpha}_1})[k]\, \beta_{\vec{\alpha}_2}(t-k).
\end{aligned} \tag{38}$$

This suggests a simple differentiation algorithm where the B-spline coefficients $c[k]$ are filtered with the digital FIR filter $d_{\vec{\alpha}_1}$ whose transfer function is given by (13) with $\vec{\alpha} = \vec{\alpha}_1$. The full procedure is summarized in Fig. 5; it includes a prefiltering step to get the B-spline coefficients of the input signal and a postfiltering with $B_{\vec{\alpha}_2}(z)$, which corresponds to the sampled version of the basis functions in (38).

D. Dilation by Integer Factors

At this stage, it is convenient to introduce the spline scaling filter, which plays an important role in our formulation:

$$H_{\vec{\alpha},m}(z) = \frac{1}{m^{N-1}} \prod_{n=1}^{N} \frac{1 - e^{m\alpha_n} z^{-m}}{1 - e^{\alpha_n} z^{-1}}. \tag{39}$$

Even though this filter is given in rational form, it turns out to be FIR of size $mN - 1$. In fact, it is not difficult to show that

$$H_{\vec{\alpha},m}(z) = \frac{1}{m^{N-1}} \prod_{n=1}^{N} \left(\sum_{k=0}^{m-1} e^{\alpha_n k} z^{-k} \right) \tag{40}$$

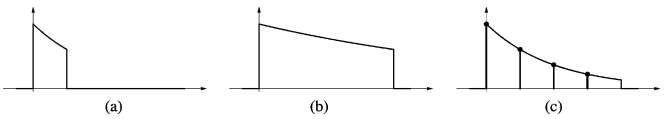

Fig. 6. Dilation versus grid coarsening. (a) Cardinal B-spline $\beta_\alpha(t)$ with $\alpha = -1/2$. (b) B-spline dilated by a factor of 4. (c) Coarse grid B-spline $\beta_{\alpha,4}(t)$ at step size $T = 4$.

so that one may think of it as a discrete analog of the exponential B-spline.

As far as scaling is concerned, the key observation is that the dilation by m (integer) of a cardinal exponential spline with parameter $\vec{\alpha}$ yields another exponential spline with knots $\{mk\}_{k\in\mathbb{Z}}$ but with a rescaled parameter $\vec{\alpha}/m$. This dilated function can also be represented as a cardinal spline by introducing artificial knots at the integers that are not multiples of m. By using the same technique as for the proof of [26, Prop. 3], we can show that the exponential B-spline with parameter $\vec{\alpha}$ satisfies the m-dilation relation

$$\beta_{\vec{\alpha}}\left(\frac{t}{m}\right) = \sum_{k\in\mathbb{Z}} h_{(\vec{\alpha}/m),m}[k]\beta_{\vec{\alpha}/m}(t-k) \tag{41}$$

where $h_{(\vec{\alpha}/m),m}[k]$ is the impulse response of the filter (39) with rescaled exponential parameter $(\alpha_1/m,\ldots,\alpha_N/m)$. The dilation relation is illustrated in Fig. 6(b) for the case of a first-order exponential B-spline. Note that the relation is compatible with the m-scale relation for causal polynomial splines, in which case, the filter $H_{(0,\ldots,0),m}(z)$ corresponds to the N-fold iteration of a moving average filter of size m [40]. The dilation relation also suggests an efficient signal processing algorithm for zooming up a signal by an integer factor of m. This algorithm, which extends the polynomial-spline method presented in [2], is schematically represented in Fig. 7. An alternative procedure proposed by Asashi *et al.* is also shown [37]. It can be shown to be equivalent to the former by using one of the Noble multirate identities (cf. [41]) to move the upsampled numerator of $H_{\vec{\alpha}/m,m}(z) = (1/m^{N-1})(\Delta_{\vec{\alpha}}(z^m)/\Delta_{\vec{\alpha}/m}(z))$ to the left-hand side of the up-sampling operator. We note, however, that the second solution is computationally less advantageous than the first one because the filter $H_{\vec{\alpha}/m,m}(z)$ is FIR of size $mN-1$. Indeed, as pointed out Vrcelj and Vaidyanathan [42] for the case of polynomial splines, the combination of upsampling and post-filtering can be implemented with N operations per output sample using the polyphase decomposition.

E. Modulation

By using the modulation property of the Fourier transform, we establish the B-spline modulation relation

$$\beta_{\vec{\alpha}}(t)\cdot e^{j\omega_0 t} = \beta_{\vec{\alpha}+\vec{j}\omega_0}(t) \tag{42}$$

where $\vec{j}$ is the N-component imaginary vector $(j,\ldots,j)$. We then use this result to show that the modulation of the spline signal $s(t) = \sum_{k\in\mathbb{Z}} c[k]\,\beta_{\vec{\alpha}}(t-k)$ yields another spline with parameter $(\alpha_1+j\omega_0,\ldots,\alpha_N+j\omega_0)$ that is given by

$$s(t)\cdot e^{j\omega_0 t} = \sum_{k\in\mathbb{Z}} c[k]\,e^{j\omega_0 k}\,\beta_{\vec{\alpha}+\vec{j}\omega_0}(t-k).$$

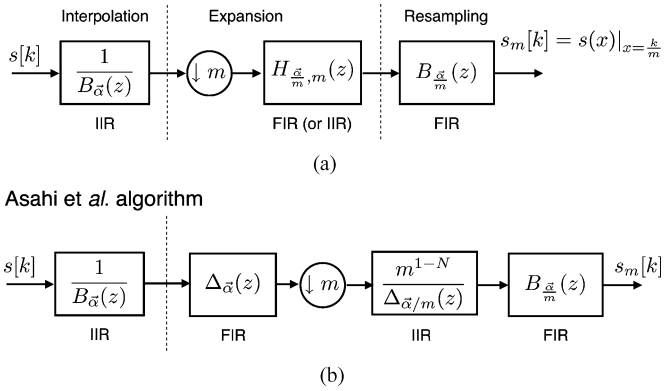

Fig. 7. Two equivalent algorithms for spline-based zooming by an integer factor of m. (a) Polynomial-spline inspired approach, which is direct transcription of the dilation relation (41). (b) Asahi *et al.* algorithm, which applies a FIR prefilter and uses a recursive IIR expansion filter.

This formula establishes an exact equivalence between the continuous-time modulation of a signal and the discrete-time modulation of its B-spline coefficients. The twist is that this also induces a corresponding change of basis functions (modulated B-splines). Note that the B-spline coefficients are unchanged when $\omega_0 = 2\pi n$, that is, when ω_0 is an even multiple of the Nyquist frequency π.

V. Multiresolution Signal Approximation

A. Exponential Spline With Knot Spacing T

By varying the knot spacing—or sampling step T—we can get finer or coarser signal representations using exponential splines. However, we observe that, in contrast with wavelet-like or polynomial-spline representations, there is no direct scaling involved (cf. Fig. 6). The underlying Green function remains the same, and it is just the spacing between the knots that is changed. The corresponding exponential B-splines are generated as in the cardinal case, except that one has to rescale the localization operator appropriately. Specifically, the B-spline with step size T is given by

$$\beta_{\vec{\alpha},T}(t) = T\cdot\Delta_{\vec{\alpha},T}\{\rho_{\vec{\alpha}}(t)\} \tag{43}$$

where the Nth-order localization operator $\Delta_{\vec{\alpha},T} = \Delta_{\alpha_1,T} * \cdots * \Delta_{\alpha_N,T}$ is constructed by iterating first-order difference operators of the form

$$\Delta_{\alpha,T}\{f(t)\} = \frac{f(t) - e^{\alpha T} f(t-T)}{T}.$$

Observe that this basis function also corresponds to the dilation by a factor of T of a cardinal B-spline with rescaled exponential parameter $(T\alpha_1,\ldots,T\alpha_N)$:

$$\beta_{\vec{\alpha},T}(t) = \beta_{T\vec{\alpha}}\left(\frac{t}{T}\right) \tag{44}$$

as may be visualized in Fig. 6(c). The equivalence between this relation and (43) becomes more apparent if we take their Fourier transform, which reads

$$\hat{\beta}_{\vec{\alpha},T}(\omega) = \frac{1}{T^{N-1}}\prod_{n=1}^{N}\frac{1-e^{\alpha_n T - j\omega T}}{j\omega-\alpha_n}. \tag{45}$$

We have now all the elements in hand to define the spline space at resolution T:

$$V_{\vec{\alpha},T} = \left\{ s(t) = \sum_{k\in\mathbb{Z}} c[k]\, \beta_{\vec{\alpha},T}(t-kT) | c \in \ell_2 \right\}. \quad (46)$$

In order to check whether or not this is a closed subspace of L_2, we need to compute the Gram sequence of the basis functions $\{\beta_{\vec{\alpha},T}(t-kT)\}_{k\in\mathbb{Z}}$. To this end, we make use of the scaling relation (43) and manipulate the inner product as follows:

$$\begin{aligned}\langle \beta_{\vec{\alpha},T}(\cdot), \beta_{\vec{\alpha},T}(\cdot - kT)\rangle &= \left\langle \beta_{T\vec{\alpha}}\left(\frac{\cdot}{T}\right), \beta_{T\vec{\alpha}}\left(\frac{\cdot}{T} - k\right)\right\rangle \\ &= T\langle \beta_{T\vec{\alpha}}(\cdot), \beta_{T\vec{\alpha}}(\cdot - k)\rangle \\ &= T \cdot a_{T\vec{\alpha}}[k]. \end{aligned} \quad (47)$$

Thus, up to a factor T, the situation is exactly the same as for the cardinal B-splines with parameter $T\vec{\alpha}$. This implies that the Riesz bounds are the ones of $\beta_{T\vec{\alpha}}(t)$ (cf. Section II) multiplied by T. Thus, we have a Riesz basis (which implies a closed subspace of L_2) if and only if $\alpha_m - \alpha_n \neq j2\pi kT^{-1}, k \in \mathbb{Z}$ for all pairs of distinct, purely imaginary roots.

In order to derive efficient approximation algorithms, it is important to investigate the embedding properties of these spline spaces. First, by using the same technique as for the derivation of (41), we obtain the m-scale relation

$$\beta_{\vec{\alpha},m}(t) = \sum_{k\in\mathbb{Z}} h_{\vec{\alpha},m}[k]\, \beta_{\vec{\alpha}}(t-k) \quad (48)$$

which relates the basis functions at step size $T = m$ to the cardinal ones at $T = 1$. More generally, we can show that

$$\beta_{\vec{\alpha},mT_0}(t) = \sum_{k\in\mathbb{Z}} h_{T_0\vec{\alpha},m}[k]\, \beta_{\vec{\alpha},T_0}(t-kT_0) \quad (49)$$

which is a relation that can be the basis for deriving fast wavelet-like approximation algorithms. A direct implication of this formula is the inclusion property $V_{\vec{\alpha},mT_0} \subset V_{\vec{\alpha},T_0}$, which holds for any positive integer m; again, this is not surprizing since the knots defining the splines in $V_{\vec{\alpha},mT_0}$ are a subset of those of $V_{\vec{\alpha},T_0}$.

B. Least-Squares Approximation

Given an arbitrary function $f(t) \in L_2$, we now consider the problem of determining its minimum-error spline approximation at resolution T. This amounts to computing its orthogonal projection into $V_{\vec{\alpha},T}$, which we denote by $\mathrm{P}_T f$. The generalized sampling theory in [36] provides an explicit form for the projection operator

$$\mathrm{P}_T f(t) = \sum_{k\in\mathbb{Z}} \langle f(\cdot), \tilde{\beta}_{\vec{\alpha},T}(\cdot - kT)\rangle_{L_2}\, \beta_{\vec{\alpha},T}(t-kT) \quad (50)$$

where the dual analysis function $\tilde{\beta}_{\vec{\alpha},T}$ is the unique function in V_T that is biorthogonal to $\beta_{\vec{\alpha},T}$, i.e., $\langle \beta_{\vec{\alpha},T}(\cdot), \tilde{\beta}_{\vec{\alpha},T}(\cdot - kT)\rangle_{L_2} = \delta_k$. By solving for this condition in the Fourier domain, we obtain

$$\begin{aligned}\hat{\tilde{\beta}}_{\vec{\alpha},T}(\omega) &= \frac{\hat{\beta}_{\vec{\alpha},T}(\omega)}{\frac{1}{T}\sum\limits_{k\in\mathbb{Z}} |\hat{\beta}_{\vec{\alpha},T}(\omega + \frac{2\pi k}{T})|^2} \\ &= \frac{\hat{\beta}_{\vec{\alpha},T}(\omega)}{T \cdot A_{T\vec{\alpha}}(e^{j\omega T})} \end{aligned} \quad (51)$$

which is guaranteed to be well-defined whenever $\beta_{\vec{\alpha},T}$ (or, equivalently, $\beta_{T\vec{\alpha}}$) satisfies the Riesz-basis condition.

We now apply this result to generate a multiresolution representation of a signal by projecting its fine-scale representation in $V_{\vec{\alpha},1}$ onto $V_{\vec{\alpha},m}$. Let $s_1(t) = \sum_{k\in\mathbb{Z}} c_1[k]\beta_{\vec{\alpha},1}(t-k)$ be our input signal and $s_m(t) = \sum_{k\in\mathbb{Z}} c_m[k]\beta_{\vec{\alpha},m}(t-mk)$ be its minimum-error approximation in $V_{\vec{\alpha},m}$. Then, we know from (50) that the B-spline coefficients of the coarse-grid signal approximation are given by

$$c_m[k] = \langle s_1(\cdot), \tilde{\beta}_{\vec{\alpha},m}(\cdot - kT)\rangle.$$

By replacing $s_1(t)$ by its B-spline expansion in the above expression, we find that the c_m's can be obtained by simple digital prefiltering and downsampling by a factor of m:

$$\begin{aligned} c_m[k] &= \sum_{k'\in\mathbb{Z}} c_1[k'] \underbrace{\left\langle \beta_{\vec{\alpha},1}(\cdot - k'), \tilde{\beta}_{\vec{\alpha},m}(\cdot - km)\right\rangle}_{\tilde{h}_{\vec{\alpha},m}[km-k']} \\ &= (c_1 * \tilde{h}_{\vec{\alpha},m})[mk] \end{aligned} \quad (52)$$

where the discrete analysis filter is defined by

$$\tilde{h}_{\vec{\alpha},m}[k] = \left\langle \beta_{\vec{\alpha}}(\cdot - k), \tilde{\beta}_{\vec{\alpha},m}(\cdot)\right\rangle.$$

Next, it is not difficult to evaluate the explicit form of this filter by moving to the Fourier domain and making use of Poisson's summation formula to identify autocorrelation terms. This gives

$$\tilde{H}_{\vec{\alpha},m}(z) = H_{\vec{\alpha}^*,m}(z^{-1}) \frac{A_{\vec{\alpha}}(z)}{m \cdot A_{m\vec{\alpha}}(z^m)}$$

with $z = e^{j\omega}$, which is an extension of the polynomial-spline solution described in [43].

The algorithmic transcription of the approximation procedure (52) and the m-scaling relation (48) yield the basic multirate Reduce and Expand operators that are shown in Fig. 8. The reduce operator coarsens the spline grid and may be used for building multiresolution signal representations. Conversely, a coarse-grid spline representation can be converted back to the finer grid by applying the Expand operator. A wavelet-like signal decomposition is obtained by considering the residuals: $c_k - \mathrm{Expand}\{\mathrm{Reduce}\{c_k\}\}$, similar to what can be done with polynomial splines [43].

Because of (49), we may also adapt the procedure for converting between grids at resolution T_0 and mT_0. However, this requires changing the exponential parameter to $\vec{\alpha}' = (T_0\alpha_1, \ldots, T_0\alpha_N)$. This is the fundamental difference with the polynomial spline case where the filters remain the same, irrespective of T_0. In fact, it is this scale invariance together with their differential properties that make polynomial splines play such a crucial role in wavelet theory [9].

C. Approximation Power of Exponential Splines

As the sampling step T gets smaller, we expect the least-squares spline approximation $\mathrm{P}_T f(t)$ to get increasingly closer to the function $f(t)$. In fact, there are general results (Jackson-type inequalities) from the theory of L-splines that indicate that the approximation error for smooth functions will decrease like the Nth power of the scale [14], [22]. In our particular setting where the grid is uniform, we can be much more precise and derive an exact asymptotic error formula.

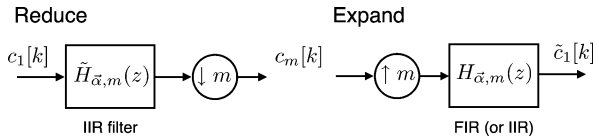

Fig. 8. Block diagram representation of the basic Reduce and Expand operators for multiresolution signal processing.

Theorem 2: Let $f \in L_2$ be a function such that $D^N f \in L_2$, and let $\mathrm{P}_T f$ denote its orthogonal projection onto the spline space $V_{\vec{\alpha},T}$ at scale T. Then, the asymptotic form of the approximation error is

$$\|f - \mathrm{P}_T f\|_{L_2} = C_N \cdot T^N \cdot \|\mathrm{L}_{\vec{\alpha}} f\|_{L_2}, \quad \text{as} \quad T \to 0 \tag{53}$$

with $C_N = \sqrt{2\zeta(2N)}/(2\pi)^N$, where $\zeta(s) = \sum_{k=1}^{\infty} 1/k^s$ is the Riemann zeta function.

The proof is given in the Appendix . This formula extends an earlier result for polynomial splines, which is essentially the same as (53), except that $\mathrm{L}_{\vec{\alpha}}$ needs to be replaced by D^N [44]. Interestingly, the asymptotic constant C_N does not depend on the precise values of the parameter vector $\vec{\alpha}$ but only on the order N. This means that the asymptotic error behavior is essentially the same for all spline approximations of order N up to a magnitude factor, which is given by $\|\mathrm{L}_{\vec{\alpha}} f\|_{L_2}$. The theorem implies that we can approximate the signal $f(t)$ as closely as we wish by taking a sampling step that is sufficiently small. However, in contrast with the classical error bounds in spline theory, our formula is quantitative and directly applicable to the determination of a critical sampling step T that guarantees that the error is below some prescribed threshold.

VI. Conclusion

In this paper, we have proposed a signal processing formulation that has allowed us to extend all the results and processing techniques available for cardinal polynomial splines to the more general family of exponential splines. We have presented the concepts using a signal processing terminology and have done our best to keep the mathematics simple (with the exception of the proof of Theorem 2). We have characterized the corresponding compactly supported B-spline basis functions and have provided exponential spline equivalents of almost all polynomial spline properties and filtering algorithms. To summarize the extension in a nutshell, this amounts to replacing polynomials by exponential polynomials, the multiple derivative operator D^N by the more general differential operator $\mathrm{L}_{\vec{\alpha}}$, and the finite differences by some exponentially weighted difference operator $\Delta_{\vec{\alpha}}$. We have also observed that there is an underlying multiresolution spline structure but that it is somewhat different from the one used in wavelet theory because it does not involve simple dilations of the B-spline basis functions.

While we believe that our treatment of the subject is fairly complete, some theoretical questions remain open. For instance, we presented no generalization of de Boor's order recursion for the calculation of B-splines [45]. It would also be interesting to know if it is possible to construct high-order B-splines that are orthogonal and if one can specify the subset of exponential parameters for which the interpolation problem is well posed. Another issue that may be relevant for real-time applications is the characterization of parameter sets for which the recursive interpolation filter is causal.

Those limitations notwithstanding, the collection of results that have been presented constitutes a foundation on which we can now build to develop specific algorithms and, more importantly, to establish new connections between the continuous- and discrete-time approaches to signal processing.

Appendix
Proof of Theorem 2

We consider the approximation of a function $f(t) \in W_2^s$ (Sobolev's space of order s) with $s \geq N$; in other words, f must be in L_2 and have $s \geq N$ derivatives in the L_2-sense. Then, from [46, Th. 1], we know that

$$\|f - \mathrm{P}_T f\|_{L_2} = \left[\int_{-\infty}^{+\infty} |\hat{f}(\omega)|^2 E_{\vec{\alpha},T}(\omega) \frac{\mathrm{d}\omega}{2\pi}\right]^{1/2} + o(T^s) \tag{54}$$

where the approximation kernel $E_{\vec{\alpha},T}$ is given by

$$E_{\vec{\alpha},T}(\omega) = \frac{\sum\limits_{k\neq 0} |\hat{\beta}_{T\vec{\alpha}}(\omega T + 2\pi k)|^2}{\sum\limits_{k\in\mathbb{Z}} |\hat{\beta}_{T\vec{\alpha}}(\omega T + 2\pi k)|^2}.$$

Since we are interested in the behavior of $\|f - \mathrm{P}_T f\|_{L_2}$ for small values of T only, we assume that $|\alpha_n T| \leq \pi/3$. To prove the theorem, we introduce the auxiliary function

$$\Psi_{k,T}(\omega) = \frac{1}{T^{2N}} \frac{|\hat{\beta}_{T\vec{\alpha}}(\omega T + 2\pi k)|^2}{\sum\limits_{k\in\mathbb{Z}} |\hat{\beta}_{T\vec{\alpha}}(\omega T + 2\pi k)|^2} \tag{55}$$

and rely on the following Lemma, which will be established below.

Lemma 1: For $k \neq 0$, the function defined by (55) satisfies the properties

$$\Psi_{k,T}(\omega) \leq |L_{\vec{\alpha}}(j\omega)|^2 \cdot \frac{1}{|k|^{2N}} \tag{56}$$

$$\lim_{T\to 0} \{\Psi_{k,T}(\omega)\} = |L_{\vec{\alpha}}(j\omega)|^2 \cdot \frac{1}{|2\pi k|^{2N}}. \tag{57}$$

Proof:

First Step: We show that for $k \neq 0$, $|\hat{\beta}_{\vec{\alpha}}(\omega + 2k\pi)| \leq M_{\vec{\alpha}}/|\pi k|^N \cdot |\hat{L}_{\vec{\alpha}}(j\omega)|$. For this, we observe that for every scalar α_n, we have the following upper bound:

$$\begin{aligned}
&\left|\frac{1 - e^{\alpha_n - j(\omega+2k\pi)}}{(j\omega - \alpha_n)(j(\omega+2k\pi) - \alpha_n)}\right| \\
&= \frac{1}{2\pi|k|}\left|\frac{1 - e^{\alpha_n - j\omega}}{j\omega - \alpha_n} - \frac{1 - e^{\alpha_n - j\omega}}{j(\omega+2k\pi) - \alpha_n}\right| \\
&= \frac{1}{2\pi|k|}\left|\hat{\beta}_{\alpha_n}(\omega) - \hat{\beta}_{\alpha_n - j2\pi k}(\omega)\right| \\
&\leq \frac{1}{2\pi|k|}\left(\sup_{\omega\in\mathbb{R}} |\hat{\beta}_{\alpha_n}(\omega)| + \sup_{\omega\in\mathbb{R}} |\hat{\beta}_{\alpha_n - j2\pi k}(\omega)|\right) \\
&\leq \frac{M_{\alpha_n}}{\pi|k|}.
\end{aligned}$$

Multiplying this inequality for $n = 1, \dots N$, we find that

$$\left| \frac{\hat{\beta}_{\vec{\alpha}}(\omega + 2k\pi)}{\prod_{n=1}^{N}(j\omega - \alpha_n)} \right| \leq \frac{M_{\vec{\alpha}}}{|\pi k|^N}$$

as we have claimed.

Second Step: We prove (56) by using the Riesz lower bound expressed by (33), namely

$$\begin{aligned} r_{T\vec{\alpha}} &\geq M_{T\vec{\alpha}} \prod_{n=1}^{N} \frac{2\cos\left(\frac{\mathrm{Im}(T\alpha_n)}{2}\right)}{\pi + |\mathrm{Im}(T\alpha_n)|} \\ &\geq \frac{M_{T\vec{\alpha}}}{\pi^N} \end{aligned}$$

taking into account that, by hypothesis, $|\alpha_n T| \leq \pi/3$. Putting things together, we finally have that

$$\Psi_{k,T}(\omega) \leq \frac{M_{T\vec{\alpha}}^2 |\hat{L}_{T\vec{\alpha}}(j\omega T)|^2}{T^{2N}|\pi k|^{2N}} \cdot \frac{1}{r_{T\vec{\alpha}}^2} \leq \frac{|\hat{L}_{\vec{\alpha}}(j\omega)|^2}{|k|^{2N}}$$

which is (56).

As for (57), we easily verify that $\lim_{T\to 0} \hat{\beta}_{T\vec{\alpha}}(\omega T) = 1$ and that $\hat{\beta}_{T\vec{\alpha}}(\omega T + 2\pi k) = T^N \hat{L}_{\vec{\alpha}}(j\omega)/(j2\pi k)^N + o(T^N)$ for $k \neq 0$ as $T \to 0$. Since $|\hat{\beta}_{T\vec{\alpha}}(\omega T + 2\pi k)|$ is bounded by an absolutely summable sequence, we can therefore claim that $\lim_{T\to 0} \sum_{k\in\mathbb{Z}} |\hat{\beta}_{T\vec{\alpha}}(\omega T + 2\pi k)|^2 = 1$, which proves (57). ■

We now consider the evaluation of the following limit, which we rewrite as

$$\lim_{T\to 0} \left\{ \frac{\|f - \mathrm{P}_T f\|_{L_2}^2}{T^{2N}} \right\} = \lim_{T\to 0} \int_{-\infty}^{+\infty} \sum_{k\neq 0} |\hat{f}(\omega)|^2 \Psi_{k,T}(\omega) \frac{\mathrm{d}\omega}{2\pi}.$$

We observe that thanks to the W_2^N-membership of f and to the bound (56), the function $g(k,\omega) = |\hat{f}(\omega)|^2 \Psi_{k,T}(\omega)$ is dominated by a summable function (in k and ω), which does not depend on T. We can thus apply Lebesgue's theorem and exchange the lim and $\int \sum$ signs, which proves that

$$\begin{aligned} &\lim_{T\to 0} \left\{ \frac{\|f - \mathrm{P}_T f\|_{L_2}^2}{T^{2N}} \right\} \\ &\quad = \int_{-\infty}^{+\infty} \sum_{k\neq 0} |\hat{f}(\omega)|^2 \lim_{T\to 0} \Psi_{k,T}(\omega) \frac{\mathrm{d}\omega}{2\pi} \\ &\quad = \int_{-\infty}^{+\infty} |\hat{f}(\omega)|^2 \sum_{k\neq 0} |L_{\vec{\alpha}}(j\omega)|^2 \frac{1}{|2\pi k|^{2N}} \frac{\mathrm{d}\omega}{2\pi} \quad \text{using (57)} \\ &\quad = C_N^2 \int_{-\infty}^{+\infty} |L_{\vec{\alpha}}(j\omega)|^2 |\hat{f}(\omega)|^2 \frac{\mathrm{d}\omega}{2\pi} \end{aligned}$$

where $C_N^2 = (2/(2\pi)^{2N})\zeta(2N)$. ■

REFERENCES

[1] M. Unser, "Splines: A perfect fit for signal and image processing," *IEEE Signal Process. Mag.*, vol. 16, no. 6, pp. 22–38, Jun. 1999.

[2] M. Unser, A. Aldroubi, and M. Eden, "Fast B-spline transforms for continuous image representation and interpolation," *IEEE Trans. Pattern Anal. Machine Intell.*, vol. 13, no. 3, pp. 277–285, Mar. 1991.

[3] ——, "B-spline signal processing: Part I—Theory," *IEEE Trans. Signal Process.*, vol. 41, no. 2, pp. 821–832, Feb. 1993.

[4] ——, "B-spline signal processing: Part II—Efficient design and applications," *IEEE Trans. Signal Process.*, vol. 41, no. 2, pp. 834–848, Feb. 1993.

[5] T. M. Lehmann, C. Gönner, and K. Spitzer, "Survey: Interpolation methods in medical image processing," *IEEE Trans. Med. Imag.*, vol. 18, no. 11, pp. 1049–1075, Nov 1999.

[6] P. Thévenaz, T. Blu, and M. Unser, "Interpolation revisited," *IEEE Trans. Med. Imag.*, vol. 19, no. 7, pp. 739–758, Jul. 2000.

[7] E. H. W. Meijering, W. J. Niessen, and M. A. Viergever, "Quantitative evaluation of convolution-based methods for medical image interpolation," *Med. Image Anal.*, vol. 5, pp. 111–126, 2001.

[8] T. M. Lehmann, C. Gönner, and K. Spitzer, "Addendum: B-spline interpolation in medical image processing," *IEEE Trans. Med. Imag.*, vol. 20, no. 7, pp. 660–665, Jul. 2001.

[9] M. Unser and T. Blu, "Wavelet theory demystified," *IEEE Trans. Signal Process.*, vol. 51, no. 2, pp. 470–483, Feb. 2003.

[10] M. Kamada, K. Toraichi, and R. E. Kalman, "A smooth signal generator based on quadratic B-spline functions," *IEEE Trans. Signal Process.*, vol. 43, no. 5, pp. 1252–1255, May 1995.

[11] L. Knockaert and F. Olyslager, "Modified B-splines for the sampling of bandlimited functions," *IEEE Trans. Signal Process.*, vol. 47, no. 8, pp. 2328–2332, Aug. 1999.

[12] S. R. Dooley, R. W. Stewart, and T. S. Durani, "Fast on-line B-spline interpolation," *Electronics Letters*, vol. 35, no. 14, pp. 1130–1131, 1999.

[13] B. P. Lathy, *Signal Process. and Linear Systems*. Carmichael, CA: Berkeley-Cambridge, 1998.

[14] L. L. Schumaker, *Spline Functions: Basic Theory*. New York: Wiley, 1981.

[15] W. Dahmen and C. A. Micchelli, "On theory and application of exponential splines," in *Topics in Multivariate Approximation*, C. K. Chui, L. L. Shumaker, and F. I. Utreras, Eds. New York: Academic, 1987, pp. 37–46.

[16] R. Panda, G. S. Rath, and B. N. Chatterjee, "Generalized B-spline signal processing," *Signal Process.*, vol. 55, pp. 1–14, 1996.

[17] I. J. Schoenberg, "Contribution to the problem of approximation of equidistant data by analytic functions," *Quart. Appl. Math.*, vol. 4, pp. 45–99, 1946.

[18] J. D. Young, "Numerical applications of hyperbolic spline functions," *Logistics Rev.*, vol. 4, pp. 17–22, 1968.

[19] B. J. McCartin, "Theory of exponential splines," *J. Approx. Theory*, vol. 66, pp. 1–23, 1991.

[20] S. Karlin and Z. Ziegler, "Chebyshevian spline functions," *SIAM J. Numer. Anal.*, vol. 3, pp. 514–543, 1966.

[21] L. L. Schumaker, "Uniform approximation by Tchebysheffian spline functions," *J. Math. Mech.*, vol. 18, pp. 369–377, 1968.

[22] J. W. Jerome, "On uniform approximation by certain generalized splines," *J. Approx. Theory*, vol. 7, pp. 143–154, 1973.

[23] A. Ron, "Exponential box splines," *Constructive Approx.*, vol. 4, pp. 357–378, 1988.

[24] ——, "Linear independence of the translates of an exponential box spline," *Rocky Mountain J. Math.*, vol. 22, pp. 331–351, 1992.

[25] C. de Boor, K. Höllig, and S. Riemenschneider, *Box Splines*. New York: Springer-Verlag, 1993.

[26] M. Unser, "Cardinal exponential splines: Part II—Think analog, act digital," *IEEE Trans. Signal Process.*, vol. 53, no. 4, pp. –, Apr. 2005.

[27] C. de Boor, *A Practical Guide to Splines*. New York: Springer-Verlag, 1978.

[28] P. M. Prenter, *Splines and Variational Methods*. New York: Wiley, 1975.

[29] G. Schweikert, "An interpolating curve using a spline in tension," *J. Math. Phys.*, vol. 45, pp. 312–317, 1966.

[30] A. M. Baum, "An algebraic approach to simply hyperbolic splines on the real line," *J. Approx. Theory*, vol. 17, pp. 189–199, 1976.

[31] I. J. Schoenberg, "On trigonometric spline interpolation," *J. Math. Mech.*, vol. 13, pp. 795–825, 1964.

[32] T. Lyche, "Trigonometric splines; a survey with new results," in *Shaping Preserving Representations in Computer-Aided Geometric Design*, J. M. Pena, Ed. Commack, NY: Nova, 1999, pp. 201–227.

[33] I. J. Schoenberg, *Cardinal Spline Interpolation*. Philadelphia, PA: SIAM, 1973.
[34] S. Mallat, *A Wavelet Tour of Signal Processing*. San Diego: Academic, 1998.
[35] M. Unser, "Sampling—50 years after Shannon," *Proc. IEEE*, vol. 88, no. 4, pp. 569–587, Apr. 2000.
[36] A. Aldroubi and M. Unser, "Sampling procedures in function spaces and asymptotic equivalence with Shannon's sampling theory," *Numer. Funct. Anal. Opt.*, vol. 15, no. 1–2, pp. 1–21, Feb. 1994.
[37] T. Asahi, K. Ichige, and R. Ishii, "A computationally efficient algorithm for exponential B-splines based on difference/IIR filter approach," *IEICE Trans. Fundam. Electron. Commun. Comput. Sci.*, vol. E85A, no. 6, pp. 1265–1273, 2002.
[38] I. J. Schoenberg, "Notes on spline functions III: On the convergence of the interpolating cardinal splines as their degree tends to infinity," *Israel J. Math.*, vol. 16, pp. 87–92, 1973.
[39] A. Aldroubi, M. Unser, and M. Eden, "Cardinal spline filters: Stability and convergence to the ideal sinc interpolator," *Signal Process.*, vol. 28, no. 2, pp. 127–138, 1992.
[40] M. Unser, A. Aldroubi, and S. J. Schiff, "Fast implementation of the continuous wavelet transform with integer scales," *IEEE Trans. Signal Process.*, vol. 42, no. 12, pp. 3519–3523, Dec. 1994.
[41] M. Vetterli and J. Kovacevic, *Wavelets and Subband Coding*. Englewood Cliffs, NJ: Prentice-Hall, 1995.
[42] B. Vrcelj and P. P. Vaidyanathan, "Efficient implementation of all-digital interpolation," *IEEE Trans. Image Process.*, vol. 10, no. 11, pp. 1639–1646, Nov. 2001.
[43] M. Unser, A. Aldroubi, and M. Eden, "The L_2 polynomial spline pyramid," *IEEE Trans. Pattern Anal. Machine Intell.*, vol. 15, no. 4, pp. 364–379, Apr. 1993.
[44] M. Unser and I. Daubechies, "On the approximation power of convolution-based least squares versus interpolation," *IEEE Trans. Signal Process.*, vol. 45, no. 7, pp. 1697–1711, Jul. 1997.
[45] C. de Boor, "On calculating with B-splines," *J. Approx. Theory*, vol. 6, pp. 50–62, 1972.
[46] T. Blu and M. Unser, "Quantitative Fourier analysis of approximation techniques: Part I—Interpolators and projectors," *IEEE Trans. Signal Process.*, vol. 47, no. 10, pp. 2783–2795, Oct. 1999.

Michael Unser (M'89–SM'94–F'99) received the M.S. (summa cum laude) and Ph.D. degrees in electrical engineering in 1981 and 1984, respectively, from the Swiss Federal Institute of Technology (EPFL), Lausanne, Switzerland.

From 1985 to 1997, he was with the Biomedical Engineering and Instrumentation Program, National Institutes of Health, Bethesda, MD. He is now Professor and Head of the Biomedical Imaging Group at EPFL. His main research area is biomedical image processing. He has a strong interest in sampling theories, multiresolution algorithms, wavelets, and the use of splines for image processing. He is the author of 100 published journal papers in these areas.

Dr. Unser is Associate Editor-in-Chief for the IEEE TRANSACTIONS ON MEDICAL IMAGING. He is on the editorial boards of several other journals, including IEEE SIGNAL PROCESSING MAGAZINE, *Signal Processing*, IEEE TRANSACTIONS ON IMAGE PROCESSING (from 1992 to 1995), and IEEE SIGNAL PROCESSING LETTERS (from 1994 to 1998). He serves as regular chair for the SPIE Conference on Wavelets, which has been held annually since 1993. He was general co-chair of the first IEEE International Symposium on Biomedical Imaging, Washington, DC, 2002. He received the 1995 and 2003 Best Paper Awards and the 2000 Magazine Award from the IEEE Signal Processing Society.

Thierry Blu (M'96) was born in Orléans, France, in 1964. He received the "Diplôme d'ingénieur" from École Polytechnique, Paris, France, in 1986 and from Télécom Paris (ENST), France, in 1988. In 1996, he received the Ph.D in electrical engineering from ENST for a study on iterated rational filterbanks applied to wideband audio coding.

He is with the Biomedical Imaging Group, Swiss Federal Institute of Technology (EPFL), Lausanne, Switzerland, on leave from the France Télécom National Center for Telecommunications Studies (CNET), Issy-les-Moulineaux, France. His research interests include (multi)wavelets, multiresolution analysis, multirate filterbanks, approximation and sampling theory, psychoacoustics, optics, wave propagation, etc.

Dr. Blu received the 2003 best paper award (SP Theory and Methods) from the IEEE Signal Processing Society. He is currently serving as an Associate Editor for the IEEE TRANSACTIONS ON IMAGE PROCESSING.